An Iterative Approach for Analyzing Wheel-Rail Interaction

Aditi Kumawat[1], Francesca Taddei[1], and Gerhard Müller[1]

[1]Chair of Structural Mechanics, TUM School of Engineering and Design, Technical University of Munich, Arcisstraße 21, 80333 Munich, Germany
{aditi.kumawat,francesca.taddei,gerhard.mueller}@tum.de

Abstract. The steady-state vehicle-track interaction or the interaction of the moving train with rail defects may result in unstable vibrations. The interaction of the moving train with such track defects induces additional dynamic stresses in the track system that may prove harmful for the structural health of the track. In this paper, a new iterative approach is proposed for analyzing the coupled equations of the vehicle-track system. The proposed approach can account for the wheel/rail contact loss. The results show that the proposed approach is computationally efficient and can be employed to study the effect of a wide range of track defects on the vehicle-track response. As an example,the vehicle-track response is obtained for the case where the wheel is traversing a rail-head corrugation. A loss of contact is observed when the wheel encounters the rail-head corrugation. The wheel-rail contact loss results in high impact loads over the rail beam leading to a sudden increase in rail beam deflections (by up to 85% and 57% for the undamped and damped cases, respectively).

Keywords: Railway track · Oscillator · Track defects.

1 Introduction

In operation, the railway track structure is subjected to motion-induced steady-state interactions as well as the arbitrarily time-varying loads caused by the interaction of a moving vehicle with various track defects. Such track defects include, e.g., vertical rail imperfections, rail discontinuities, and local track irregularities. To study the effects of time-dependent loads caused by track defects, the railway track structure is commonly analyzed with the help of various numerical and analytical models [6,7].

Further aspects of vehicle-track interaction modelling are the idealization of the vehicle system and the evaluation of the time-dependent loads caused by the interaction of a moving vehicle with the track. Usually, two frameworks are followed for the idealization of the vehicle system. In the first framework, the vehicle is idealized as a point force with a magnitude equal to the axle load. This idealization, where the inertial and internal degrees of freedom of the vehicle are neglected, is more suited for studying the dynamic behaviour of

the track itself or wave propagation analysis in the soil medium underlying the track [11]. In the second framework, the degrees of freedom of the vehicle are duly considered by modelling the vehicle as a moving mass [16,20], a single or multi-degree-of-freedom (SDOF or MDOF) moving oscillator system [3,17], or as a multi-degree-of-freedom lumped mass model [11,19].

A commonly used vehicle idealization that can account for the inertia and the degrees of freedom of the vehicle is the 'moving oscillator models'. It may be mentioned that the more accurate representation of the vehicle system is by MDOF systems (in comparison to SDOF systems), where the masses can represent both the unsprung (wheel) and sprung masses of the vehicle (bogie, car body). Further, the primary and secondary suspension systems of the vehicle can be represented via spring-damper systems. For evaluating the time-dependent loads due to the moving oscillator, a coupling is established between the governing equations of the oscillator and track model via a pre-defined wheel-rail contact model (e.g., permanent, linear, nonlinear contact models). In some studies, the coupled equations of motion associated with the vehicle-track system are solved by using analytical method [3], modified numerical integration techniques [13,14,15], and finite element method [4,17]. In addition to that, this problem has also been investigated by employing the Green's function [21,12,10] derived using the conventional frequency-domain approach.

A recent study by Dimitrovová [3] has shown that it is also possible to analyze the moving oscillator problem using a semi-analytical approach. In their study, the beam deflections are evaluated for beam on the viscoelastic-Pasternak model under one and two mass uniformly moving oscillators. The solution is presented as a sum of the steady-state part (derived analytically), induced harmonic part (derived semi-analytically), and transient part (derived numerically). However, it may be noted that the proposed solution is only applicable to the permanent wheel-rail contact model. For more complex vehicle-track models that take into account the possibility of contact loss, most studies tend to use numerical approaches [1,18]. Those numerical approaches are in general cumbersome and, in some cases, computationally intensive [1].

In this study, a new analytical iterative approach is presented to analyze the coupled equation of motion of the vehicle-track system. The vehicle is modeled as a multi-degree-of-freedom system moving on a one-dimensional track model. The proposed approach is validated with the above-described analytical study [3]. The results show the vehicle-track response for three cases. In the first case, the wheel (unsprung mass) remains in permanent contact with the rail beam. In the second case, the wheel interacts with the rail via a nonlinear Hertzian spring. In the third case, in addition to modeling the wheel-rail interaction using the Hertzian spring, the wheel is considered to be moving over a rail-head corrugation.

2 The Iterative Approach

2.1 Track model

The model used to idealize and study the behaviour of the railway track system is shown in Figure 1. The rail beam is modeled as an infinite Euler-Bernoulli beam (with x denoting the space coordinate measured along the length of the rail beam) overlying a two-parameter foundation model consisting of (1) Pasternak shear layer of thickness H_P and shear modulus G_P per unit beam length and (2) viscoelastic Winkler spring layer with K_0 denoting the spring stiffness per unit beam length. The model is subjected to a time-varying vertical force $P(t)$ resulting due to interaction between the rail beam and a multi-degree-of-freedom (MDOF) oscillator system moving with uniform velocity v.

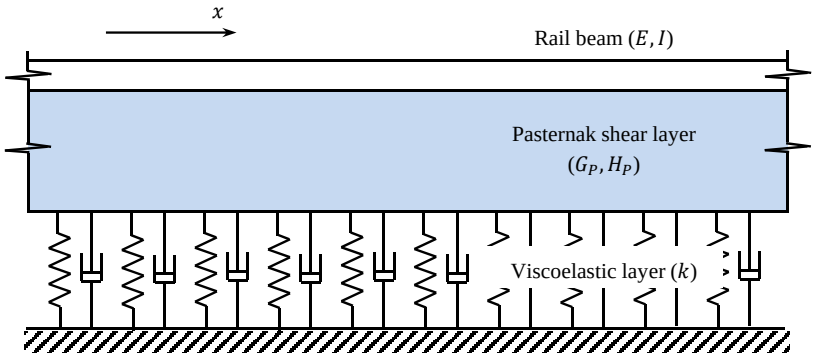

Fig. 1: Definition sketch of the model idealizing railway track section.

Under the above-described idealizations, the equation of motion of a rail beam is described by [8]

$$EI\frac{\partial^4 w}{\partial x^4} - K_1\frac{\partial^2 w}{\partial x^2} + K_0 w + c\frac{\partial w}{\partial t} + \rho\frac{\partial^2 w}{\partial t^2} = P(t)\delta(x - vt) \tag{1}$$

where $w(x,t)$ is the transverse deflection of the rail beam (considered positive downwards), E is the Young's modulus of rail beam material, I is the moment of inertia of the rail beam cross-section about the axis of bending, $K_1 = (G_P H_P)$ is the shear parameter associated with the Pasternak shear layer, ρ is the mass per unit length of the beam, c is the coefficient of viscous damping per unit beam length, and δ is the Dirac's delta function.

Denoting $\iota = \sqrt{-1}$ and $\hat{f}(\omega)$ as the Fourier transform of an arbitrary time-varying function $f(t)$ can be expressed as,

$$\hat{f}(\omega) = \int_{-\infty}^{\infty} f(t) e^{-\iota\omega t} dt \tag{2}$$

$$f(t) = \frac{1}{2\pi}\int_{-\infty}^{\infty} \hat{f}(\omega) e^{\iota\omega t} d\omega \tag{3}$$

On taking Fourier transform of Equation 1 (assuming that $w(x,t)$ and its time derivatives vanish at $t = \pm\infty$) using Equation 2 and solving for the rail beam deflection $\widehat{w}\,(x,\omega)$ in space-frequency-domain, we obtain,

$$\widehat{w}\,(x,\omega) = \left(\frac{P(x/v)v^3}{EI\omega^4 + K_1\omega^2 v^2 + K_0 v^4 - \rho\omega^2 v^4 + \iota c\omega v^4}\right) e^{-i\omega\left(\frac{x}{v}\right)} \tag{4}$$

Further, using Equations 4 and 3 the expression for the rail-beam deflection $w_0(t) = w(vt,t)$ at the point of contact with the load $P(t)$ can be written in a concise form as

$$w_0(t) = \frac{P\,(t)}{2\pi} I(v,t) \tag{5}$$

where

$$I(v,t) = \int_{-\infty}^{\infty} \frac{v^3 d\omega}{EI\omega^4 + K_1\omega^2 v^2 + K_0 v^4 - \rho\omega^2 v^4 + \iota c\omega v^4} \tag{6}$$

here ω stands for frequency. The mathematical technique exponential window method [5] is employed while evaluating the above integral.

2.2 Vehicle Model

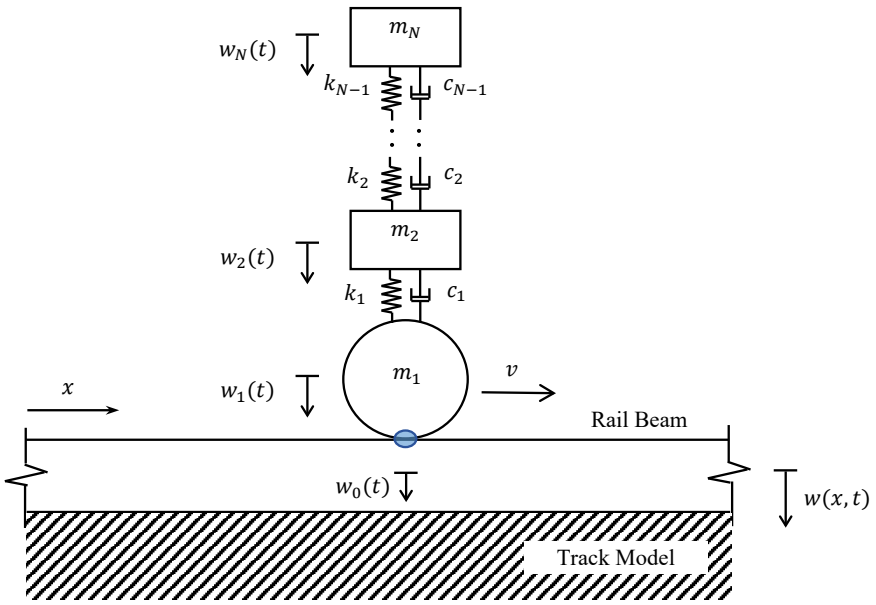

Fig. 2: MDOF oscillator moving over the track model with no loss of contact.

Figure 2 shows the considered oscillator system comprising N masses (m_1, m_2,...,m_N), connected via $N-1$ springs (of stiffness, $k_1, k_2, ..., k_{N-1}$), and $N-1$ dash-pot systems (with viscous damping coefficients, $c_1, c_2, ..., c_{N-1}$). Further, $(w_i)_{i=1\ to\ N}$ respectively represent the absolute displacements of the masses $(m_i)_{i=1\ to\ N}$. The contact between the oscillator and the rail beam is such that the unsprung mass m_1 always remains in contact with the rail beam (see Figure 2),

$$w_1(t) = w_0(t) \tag{7}$$

On considering the vertical equilibrium of the mass m_1 and using Equations 5 and 7 the displacements w_1 (of the unsprung mass m_1 or rail beam) and w_2 (of the sprung mass m_2) can be related as

$$m_1\ddot{w}_1 + \left(k_1 + \frac{2\pi}{I(T_P, v)}\right) w_1 + c_1\dot{w}_1 = k_1 w_2 + c_1\dot{w}_2 + P_0 \tag{8}$$

here $P_0 = (m_1 + m_2 + ... + m_N)g$ (where, g is the acceleration due to gravity) is the static load which is considered equal to the total weight of the oscillator. Furthermore, on considering the vertical equilibrium of the forces acting on the sprung masses ($m_2,\ m_3, ..., m_N$) of the oscillator system following expression can be written

$$\mathbf{m}\ddot{\mathbf{w}}(t) + \mathbf{k}\mathbf{w}(t) + \mathbf{c}\dot{\mathbf{w}}(t) = \mathbf{f}(t) \tag{9}$$

where $\mathbf{w}(t) = \{w_2(t),\ w_3(t), \ldots, w_N(t)\}^T$ is the displacement vector and, $\dot{\mathbf{w}}(t)$ and $\ddot{\mathbf{w}}(t)$ respectively denote the corresponding velocity and acceleration vectors of the sprung masses ($m_2,\ m_3, ..., m_N$). Further, $\mathbf{m}$, $\mathbf{k}$, and $\mathbf{c}$ are respectively the mass, stiffness, and damping matrices, and the column vector $\mathbf{f}(t)$ representing the forces acting on the sprung masses is given by,

$$\mathbf{f}(t) = \begin{Bmatrix} k_1 w_1 + c_1\dot{w}_1 \\ 0 \\ \vdots \\ 0 \end{Bmatrix} \tag{10}$$

It may be noted that Equation 9 is a set of $N-1$ coupled differential equations governing the displacements $\mathbf{w}(t)$ resulting due to forces $\mathbf{f}(t)$. This system possess $N-1$ classical natural modes ϕ_n corresponding to $N-1$ natural vibration frequencies ω_n, where n describes the mode number ($n = 2,\ 3, ...,\ N$). Furthermore, those $N-1$ natural modes can be written in the form of a modal matrix $\mathbf{\Phi}$ as,

$$\mathbf{\Phi} = \left[\phi_{jn}\right] \tag{11}$$

where j indicates the degrees of freedom ($j = 2,\ 3, ...,\ N$). Further, using the modal matrix, the displacement vector can be represented in the following form

$$\mathbf{w}(t) = \mathbf{\Phi}\mathbf{q}(t) \tag{12}$$

where $\mathbf{q}(t) = \{q_2(t),\ q_3(t), \ldots,\ q_N(t)\}^T$ are the modal coordinates.

Further, the classical modal analysis procedure [2] is used to transform the equation of motion for the sprung masses (see Equation 9) to N uncoupled differential equations in modal coordinates $\mathbf{q}(t)$, described by

$$\mathbf{M}\ddot{\mathbf{q}}(t) + \mathbf{K}\mathbf{q}(t) + \mathbf{C}\dot{\mathbf{q}}(t) = \mathbf{F}(t) \tag{13}$$

where, $\mathbf{M}$, $\mathbf{K}$, and $\mathbf{C}$ are diagonal matrices given by

$$\mathbf{M} = \mathbf{\Phi}^T\mathbf{m}\mathbf{\Phi} \qquad \mathbf{K} = \mathbf{\Phi}^T\mathbf{k}\mathbf{\Phi} \qquad \mathbf{C} = \mathbf{\Phi}^T\mathbf{c}\mathbf{\Phi} \tag{14}$$

and the vector $\mathbf{F}(t)$ as,

$$\mathbf{F}(t) = \mathbf{\Phi}^T\mathbf{f}(t) \tag{15}$$

The uncoupled, modal differential equations (see Equation 13) can be solved to find the modal responses $\mathbf{q}(t)$, which are then combined to determine the displacement response $\mathbf{w}(t)$ using Equation 12.

It may be observed from Equations 9 and 10 that $\mathbf{w}(t)$ is dependent on $w_1(t)$. Furthermore, as seen from Equation 8, $w_1(t)$ itself depends on $w_2(t)$ (and hence on $\mathbf{w}(t)$). To solve this coupled system of equations governing the displacement responses $w_1(t)$ (or $w_0(t)$) and $\mathbf{w}(t)$ a two-step iterative scheme is employed. In the first step, $\mathbf{w}(t)$ (or $w_2(t)$) is determined using Equations 9–15 for a given $w_1(t)$ (or $w_0(t)$). In the second step, the above-evaluated $w_2(t)$, is used to find $w_1(t)$ using Equation 8. These two steps are repeated until the respective values of $w_1(t)$ and $\mathbf{w}(t)$ converges.

Figure 3 illustrates the steps of the proposed iterative scheme via a flowchart. In this figure, the variables k and $\epsilon(t)$ represent the iteration number and required precision, respectively. It may be noted that for the first iteration ($k = 1$), $w_0(t) = w_1(t) = 0$ is used.

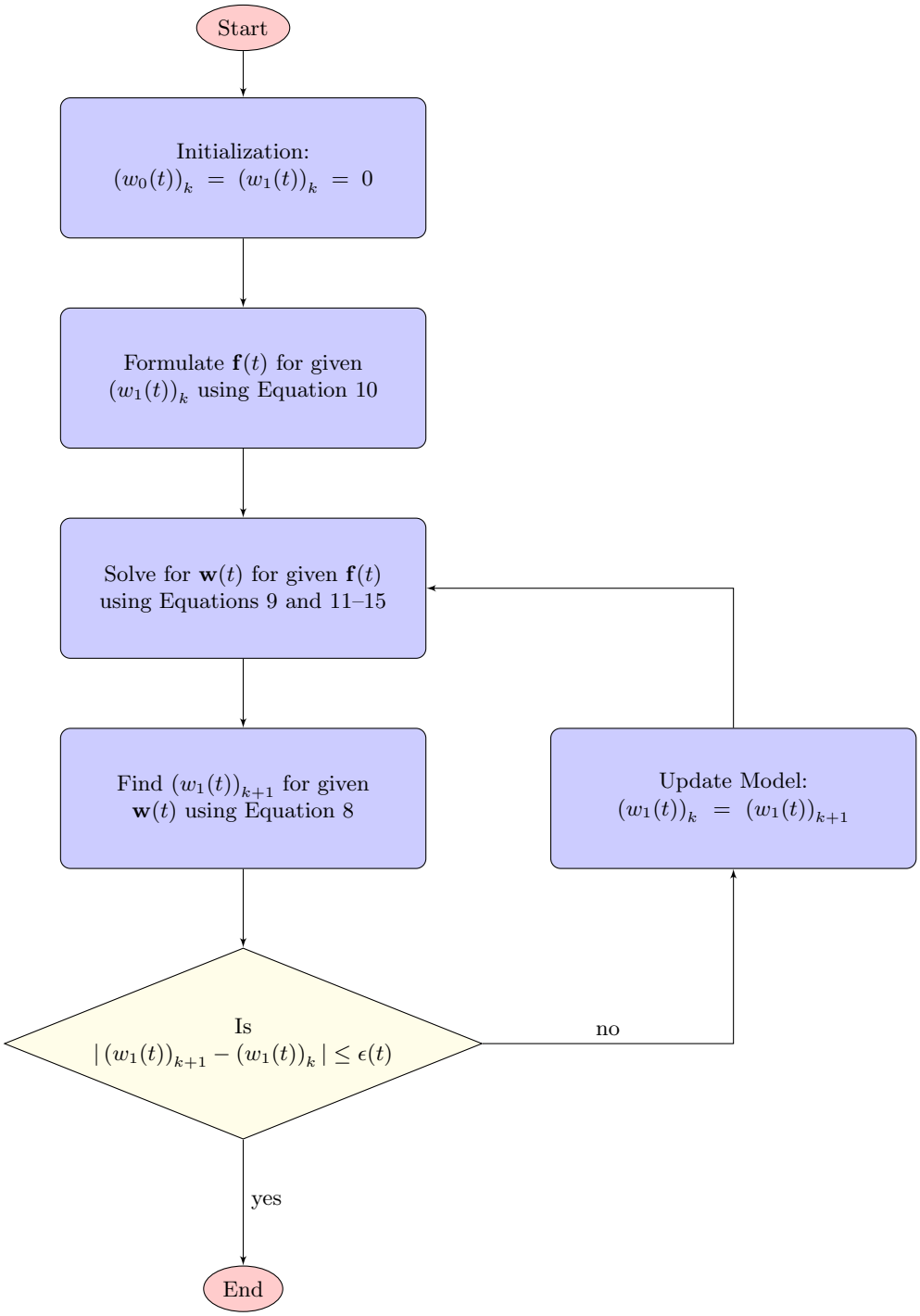

Fig. 3: Flow chart showing the steps of the iterative approach used for analyzing the track model traversed by a MDOF system (k and $\epsilon(t)$ represent the iteration number and required precision, respectively).

3 Validation of the proposed approach

The results show the response analysis of a MDOF oscillator comprising three masses (m_1, m_2, and m_3) connected via two springs (of stiffness k_1 and k_2) and two dash-pot systems (with viscous damping coefficients, c_1 and c_2) moving uniformly over the rail beam overlying the Pasternak-viscoelastic model. The track and oscillator parameters used for this analysis are given in Table 1.

Before analysing the vibration responses of the MDOF oscillator, a validation

Table 1: Track and oscillator parameters [9,12]

Parameter	Value
Rail Beam	
Mass per unit beam length, ρ	60 kg/m
Modulus of Elasticity of rail, E	210 GPa
Central moment of Inertia of rail, I	3055 cm^4
Pasternak Layer	
Shear Modulus, G_P	43.3 MPa
Height, H_P	0.3 m
Viscoelastic Layer	
Stiffness, K_0	4.08 MPa
Coefficient of viscous damping, c	1.56 kNs/m
Oscillator	
Lower Mass, m_1	1125 kg
Middle Mass, m_1	2000 kg
Upper Mass, m_1	6875 kg
Stiffness of lower connecting spring, k_1	6.3 MN/m
Stiffness of upper connecting spring, k_2	390 kN/m
Coefficient of viscous damping of lower connecting dashpot, c_1	23 kNs/m
Coefficient of viscous damping of upper connecting dashpot, c_2	20 kNs/m
Hertz's constant, C_H	98.92 $GN/m^{3/2}$

exercise is carried out. The proposed approach is implemented to find the deflection response of a mass-spring system with mass m_1 and stiffness k_1 (see Table 1) traversing the rail beam overlying a viscoelastic layer ($G_P = 0$) with velocity v=100 m/s (see Fig. 4). It is assumed that there is no loss of contact between the mass-spring system and rail beam. Fig.5 compares the normalized deflection values of the rail beam at the position of the moving mass-spring system ($\overline{w}_0(t)$), and that of mass m_1 ($\overline{w}_1(t)$) obtained using the proposed approach with those evaluated using a recently proposed analytical solution by Dimitrovová [3]. The deflection values (w_1 and w_0) are normalized with respect to the rail beam deflection value, $w_0(t) = (m_1 g/2\pi)I(T_P, v)$ (see Eq.(5)), where, g is the acceleration due to gravity. The agreement between the vibration responses evaluated using the two approaches lends confidence in the proposed approach. The validation shown in this section is for a single-mass oscillator deflection solution compared

to the rail and mass-deflection obtained using semi-analytical approach shown in Dimitrovová [3]. It may be mentioned that this a partial comparison and can be extended for case of the two-mass moving oscillator.

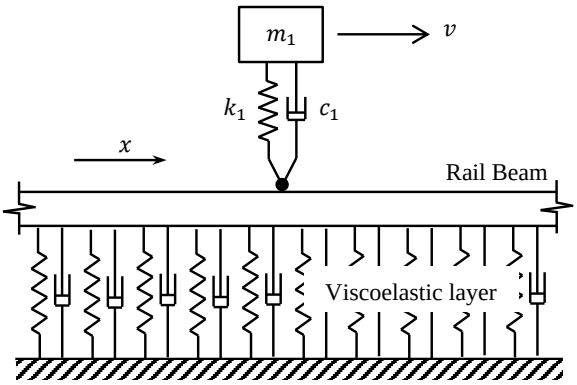

Fig. 4: MDOF oscillator moving over the track model with no loss of contact.

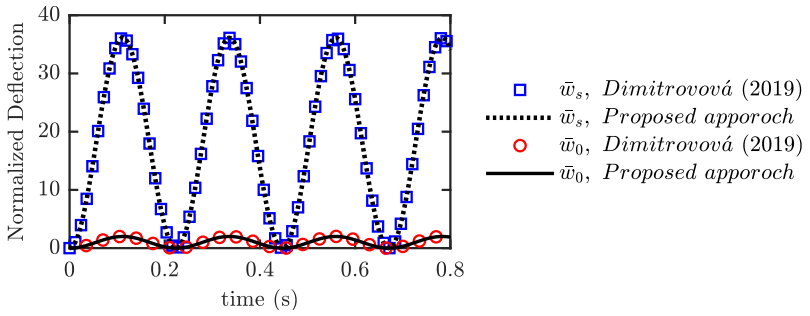

Fig. 5: Comparison of the normalized rail beam deflection ($\bar{w}_0$) and normalized oscillator deflections ($\bar{w}_1$) computed using the proposed approach and analytical solution by Dimitrovová [3].

4 Wheel-Rail Contact Loss

In previous sections it is assumed that the moving oscillator system (see Figure 2) never loses contact with the rail beam. However, for more realistic modelling of vehicle-track interaction it is essential to consider the wheel-rail contact loss. The complex vehicle-track models that take into account the possibility of contact loss tend to use numerical approaches. Those approaches are generally based on time integration (via Newmark-β, Runge-Kutta, or precise integration methods) of the equation of motion derived from the finite element vehicle-track models [1,18]. In this section, it is assumed that the wheel interacts with the rail via a nonlinear Hertzian spring (see Figure 6). The track model is same as shown in Figure 1.

For analyzing this system, the equation relating the rail beam deflection $w_0(t)$ to the load $P(t)$ acting on the rail beam (see Equation 5) is modified as,

$$\left(\frac{P(t)}{C_H}\right)^{2/3} = \xi(t) H\left[\xi(t)\right] \tag{16}$$

where, C_H is the Hertz's constant, $H(.)$ is the Heaveside function, and

$$\xi(t) = w_1(t) - w_0(t) - z(t) \tag{17}$$

here $z(t)$ denotes the rail or wheel roughness.

Using the proposed iterative approach, the response analysis of the moving MDOF oscillator comprising three masses (see Figure 6) is performed for three different cases. In the first case, the wheel (unsprung mass) always remains in contact with the rail beam. In the second case, the wheel interacts with the rail via a nonlinear Hertzian spring. In the third case, in addition to modelling the wheel-rail interaction using the Hertzian spring, the MDOF oscillator is considered to be moving over a rail-head corrugation (see Equations 16 and 17) of the form,

$$z(t) = -\frac{e}{2}\left(1 - \cos(2\pi v t)\right), \qquad \frac{x_{z_1}}{v} \leq t \leq \frac{x_{z_2}}{v} \tag{18}$$

where e represents the depth of the rail indentation, and x_{z_1} and x_{z_2} respectively denote the start and end locations of the rail corrugations along the length of the rail beam. Further, each of the above case is analyzed considering both the undamped and damped oscillator systems. The track parameters and oscillator parameters are shown in Table 1. The vertical deflections of the rail beam ($w_0(t)$) and those of the masses m_1 ($w_1(t)$), m_2 ($w_2(t)$), and m_3 ($w_3(t)$) are evaluated at the location $x = vt$. It is assumed that the oscillator is at rest and all deflections values are zero at the location $x = 0$ and time $t = 0$. Further, the computed deflection values are normalized by the rail beam deflection value, $w_0(t) = (P_0/2\pi)I(T_P, v)$ (see Equation 5), where $P_0 = (m_1 + m_2 + m_3)g$.

Figures 7 and 8 show the normalized deflection $\overline{w}_0(t))$, $\overline{w}_1(t)$, $\overline{w}_2(t))$, and $\overline{w}_3(t)$ with time t for the above-mentioned cases of wheel-rail contact undamped and damped oscillator systems, respectively. Here, the oscillator velocity is considered as $v = 100$ m/s and, for illustration, the rail corrugation depth, start and end locations are respectively chosen as, $e = 0.35$ mm, $x_{z_1} = 20$ m, and $x_{z_2} = 40$ m (see Equation 18). For both figures, parts, (a), (b), and (c) respectively correspond to the cases of (1) no loss of wheel-rail contact, (2) Hertzian wheel-rail contact, and (3) wheel moving over a rail-head corrugation (see Equation 18).

It may be observed for both the considered cases of wheel-rail contact (no loss of contact and Hertzian) that introduction of damping into the oscillator results in the decay of deflection amplitudes of the rail beam as well as that of the oscillator masses. Moreover, it is interesting to note that the damping brings the normalized rail beam deflection closer to $\overline{w}_0$ =1, i.e., the deflection value observed if a point load of magnitude P_0 moves over the rail beam with velocity $v = 100$ m/s.

Further, it is found that the idealisation of wheel-rail contact via a Hertzian spring (see Figures 7b and 8b) leads to slightly higher amplitude (by up to 8%) of the rail beam deflection as compared to those observed for the case where there is no loss of wheel-rail contact (see Figures 7a and 8a). Similar behaviour is observed for the deflection responses $(\overline{w}_1(t))$, $\overline{w}_2(t))$, and $\overline{w}_3(t))$ of the oscillator masses m_1, m_2, and m_3.

It may also be seen that similar to the case of no wheel-rail contact loss (see Figures 7a and 8a), the unsprung mass m_1 remains in contact with the rail beam even for the case of Hertzian contact (see Figures 7b and 8b). However, a loss of contact is observed when the oscillator encounters the rail-head corrugation at t =0.2 s (see Figures 7c and 8c). The wheel-rail contact loss results in high impact loads over the rail beam leading to a sudden increase in rail beam deflections (by up to 85% and 57% for the undamped and damped cases, respectively). It may be noted that the time required for the evaluation of the deflection responses shown in Figure 7c on a a personal computer (with 8 GB RAM and 3.40 GHz quad-core Intel i5 processor) is $\sim$40 s.

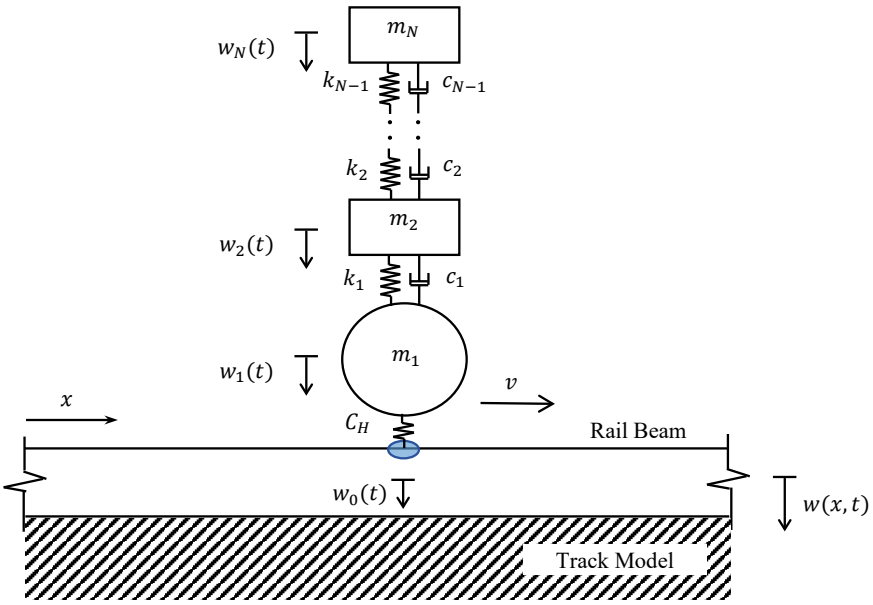

Fig. 6: MDOF oscillator moving over the track model with nonlinear Hertzian contact.

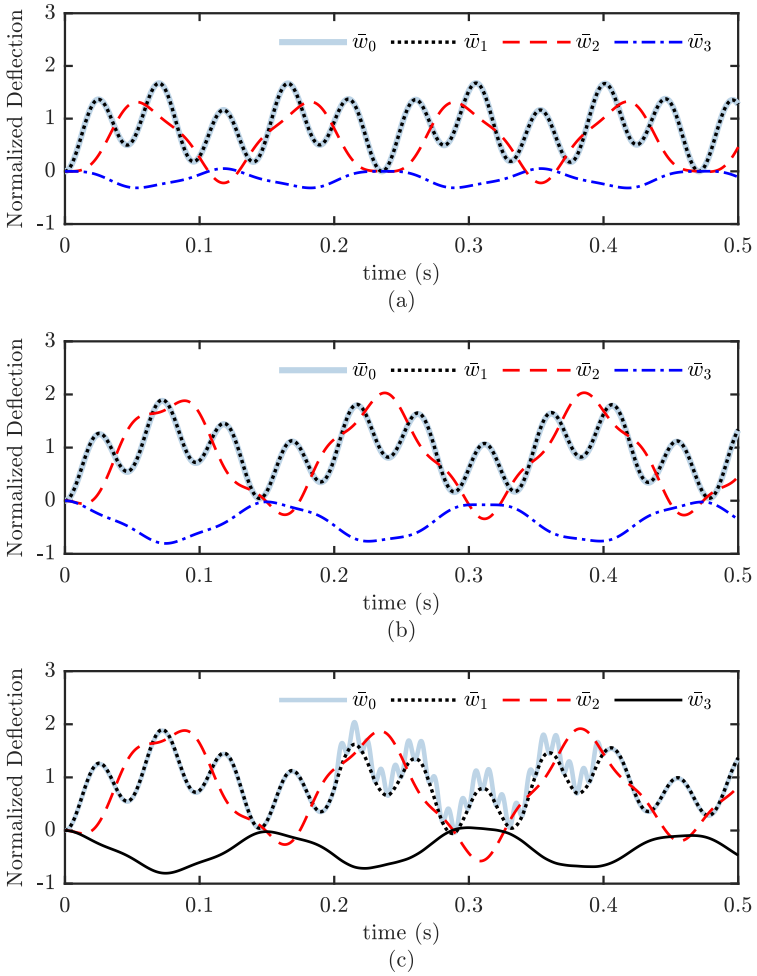

Fig. 7: Normalized deflections of the rail beam ($\overline{w}_0(t)$), and masses m_1 ($\overline{w}_1(t)$), m_2 ($\overline{w}_2(t)$), and m_3 ($\overline{w}_3(t)$) with time t at location $x = vt$ ($v = 100$ m/s) of an undamped oscillator system for the cases of (a) no loss of wheel-rail contact, (b) Hertzian wheel-rail contact, (c) rail-head corrugation.

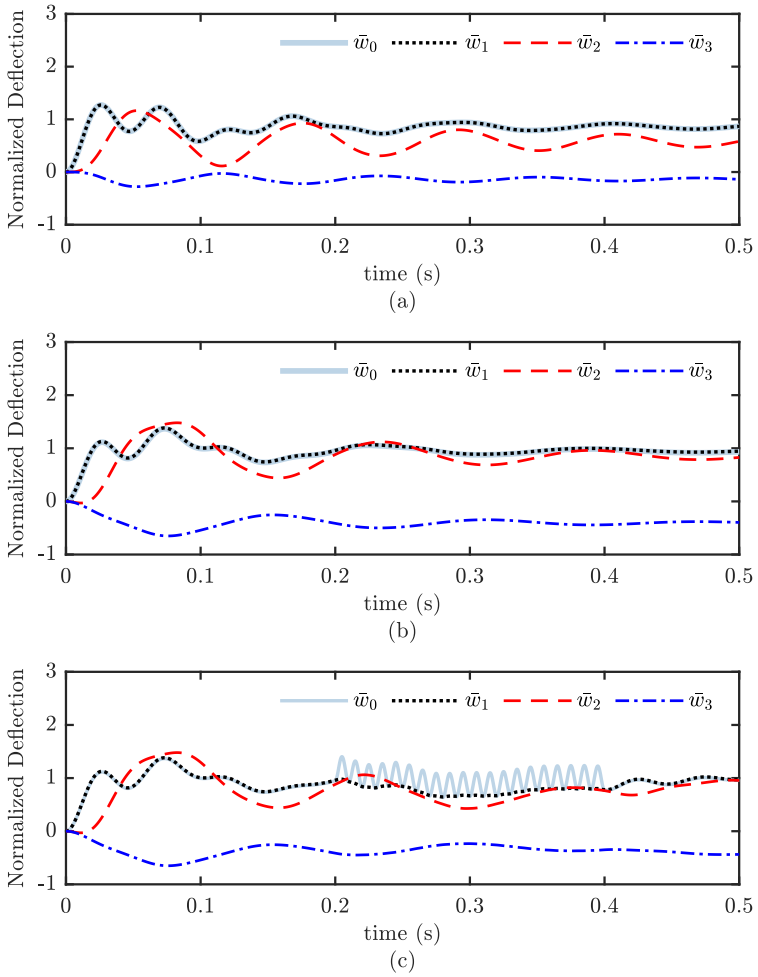

Fig. 8: Normalized deflections of the rail beam ($\overline{w}_0(t)$), and masses m_1 ($\overline{w}_1(t)$), m_2 ($\overline{w}_2(t)$), and m_3 ($\overline{w}_3(t)$) with time t at location $x = vt$ ($v = 100$ m/s) of an damped oscillator system for the cases of (a) no loss of wheel-rail contact, (b) Hertzian wheel-rail contact, (c) rail-head corrugation.

5 Conclusions

A new iterative approach is proposed for investigating the effect of various track defects on vehicle-track response. It is found that this approach is computationally efficient and can be implemented for analyzing different cases of wheel-rail contact, namely, permanent wheel-rail contact and linear and nonlinear Hertzian wheel-rail contact. As an example, the vehicle-track response is obtained for the case when the wheel is traversing a rail-head corrugation. A loss of contact is observed when the wheel encounters the rail-head corrugation. It is found that the wheel-rail contact loss results in high impact loads over the rail beam leading to a sudden increase in rail beam deflections (by up to 85% and 57% for the undamped and damped cases, respectively). The proposed approach can be extended for a more complex vehicle model with multiple wheel-rail contacts. Furthermore, by implementing the track's Green function [9], one can quickly evaluate the rail-beam response at any other track location. Finally, it is essential to highlight that the contemporary analytical approaches available for analyzing the moving-oscillator problem can only evaluate the rail and oscillator deflection for the case where there is no loss of wheel-rail contact. On the other hand, the presented approach can incorporate the nonlinear wheel-rail contact model and consider the possibility of wheel-rail contact loss.

References

1. Baeza, L., Roda, A., Nielsen, J.C.: Railway vehicle/track interaction analysis using a modal substructuring approach. Journal of sound and vibration **293**(1-2), 112–124 (2006)
2. Chopra, A.K., et al.: Dynamics of structures. Pearson Education Upper Saddle River, NJ (2012)
3. Dimitrovová, Z.: Semi-analytical solution for a problem of a uniformly moving oscillator on an infinite beam on a two-parameter visco-elastic foundation. Journal of Sound and Vibration **438**, 257–290 (2019)
4. Hino, J., Yoshimura, T., Konishi, K., Ananthanarayana, N.: A finite element method prediction of the vibration of a bridge subjected to a moving vehicle load. Journal of Sound and Vibration **96**(1), 45–53 (1984)
5. Kausel, E., Roësset, J.M.: Frequency domain analysis of undamped systems. Journal of Engineering Mechanics **118**(4), 721–734 (1992)
6. Knothe, K., Grassie, S.: Modelling of railway track and vehicle/track interaction at high frequencies. Vehicle system dynamics **22**(3-4), 209–262 (1993)
7. Kouroussis, G., Connolly, D.P., Verlinden, O.: Railway-induced ground vibrations–a review of vehicle effects. International Journal of Rail Transportation **2**(2), 69–110 (2014)
8. Kumawat, A., Raychowdhury, P., Chandra, S.: Frequency-dependent analytical model for ballasted rail-track systems subjected to moving load. International Journal of Geomechanics **19**(4), 04019016 (2019)
9. Kumawat, A., Raychowdhury, P., Chandra, S.: A wave number based approach for the evaluation of the green's function of a one-dimensional railway track model. European Journal of Mechanics-A/Solids **78**, 103854 (2019)
10. Mazilu, T.: Instability of a train of oscillators moving along a beam on a viscoelastic foundation. Journal of Sound and Vibration **332**(19), 4597–4619 (2013)
11. Mazilu, T.: Interaction between moving tandem wheels and an infinite rail with periodic supports–green's matrices of the track method in stationary reference frame. Journal of Sound and Vibration **401**, 233–254 (2017)
12. Mazilu, T., Dumitriu, M., Tudorache, C.: Instability of an oscillator moving along a timoshenko beam on viscoelastic foundation. Nonlinear Dynamics **67**(2), 1273–1293 (2012)
13. Muscolino, G., Benfratello, S., Sidoti, A.: Dynamics analysis of distributed parameter system subjected to a moving oscillator with random mass, velocity and acceleration. Probabilistic Engineering Mechanics **17**(1), 63–72 (2002)
14. Muscolino, G., Palmeri, A.: Response of beams resting on viscoelastically damped foundation to moving oscillators. International Journal of Solids and structures **44**(5), 1317–1336 (2007)
15. Muscolino, G., Palmeri, A., Sofi, A.: Absolute versus relative formulations of the moving oscillator problem. International Journal of Solids and Structures **46**(5), 1085–1094 (2009)
16. Patil, S.P.: Response of infinite railroad track to vibrating mass. Journal of engineering mechanics **114**(4), 688–703 (1988)
17. Rodrigues, C., Simões, F.M., da Costa, A.P., Froio, D., Rizzi, E.: Finite element dynamic analysis of beams on nonlinear elastic foundations under a moving oscillator. European Journal of Mechanics-A/Solids **68**, 9–24 (2018)
18. Sadeghi, J., Khajehdezfuly, A., Esmaeili, M., Poorveis, D.: Investigation of rail irregularity effects on wheel/rail dynamic force in slab track: comparison of two and three dimensional models. Journal of Sound and Vibration **374**, 228–244 (2016)

19. Sun, Y.Q., Dhanasekar, M.: A dynamic model for the vertical interaction of the rail track and wagon system. International Journal of Solids and Structures **39**(5), 1337–1359 (2002)
20. Visweswara Rao, G.: Linear dynamics of an elastic beam under moving loads. J. Vib. Acoust. **122**(3), 281–289 (2000)
21. Yang, B., Tan, C., Bergman, L.: Direct numerical procedure for solution of moving oscillator problems. Journal of engineering mechanics **126**(5), 462–469 (2000)